CONEM 2022
CONGRESSO NACIONAL DE ENGENHARIA MECÂNICA
TERESINA - PI

ABCM
XI CONGRESSO NACIONAL DE ENGENHARIA MECÂNICA
DE 07 A 11 DE AGOSTO DE 2022, TERESINA-PI, BRASIL

INFLUENCE OF MEMBRANE EFFECTIVE THERMAL CONDUCTIVITY AND TORTUOSITY MODELS ON THE PERFORMANCE OF DCMD SYSTEMS FOR DESALINATION

Ingrid Vasconcelos Curcino, ingrid.curcino@mecanica.coppe.ufrj.br [1]
Paulo Roberto Siqueira Costa Júnior, paulorobertoscj@gmail.com [2]
Abdul Orlando Cárdenas Gómez, orlandocardenas1589@gmail.com [1]
Luz Elena Peñaranda Chenche, Ing.elenap@gmail.com [1]
João Alves de Lima, jalima@cear.ufpb.br [1,3]
Carolina Palma Naveira-Cotta, carolina@mecanica.coppe.ufrj.br [1]
Renato Machado Cotta, cotta@mecanica.coppe.ufrj.br [1,4]

[1]Laboratory of Nano & Microfluidics and Microsystems - LabMEMS, Mechanical Eng. Dept., POLI & COPPE/UFRJ, Rio de Janeiro, RJ, Brazil
[2]Wikki Brasil LTDA, Technological Park, Federal University of Rio de Janeiro, Rio de Janeiro, RJ, Brazil.
[3]Renewable Eng. Dept., DEER/CEAR, Federal University of Paraíba, João Pessoa, PB, Brazil.
[4]General Directorate of Nuclear and Technological Development, DGGDNTM, Brazilian Navy, Rio de Janeiro, RJ, Brazil.

Abstract. *The Direct Contact Membrane Distillation (DCMD) is a thermally driven membrane separation process pointed out as a promising alternative for seawater desalination from low exergy waste heat recovery. The development of proper mathematical models for describing the effects of the characteristics of microporous and hydrophobic membranes, which act as a non-wetting barrier in the membrane distillation (MD) process, is necessary for a robust analysis of the process. This study aims to analyze membrane effective thermal conductivity (resistances in parallel, series, and Maxwell I) and tortuosity (Euclidian and fractal approaches) models that can be used to calculate membrane effective and morphological properties. For this purpose, simulated values of distillate mass flux were obtained from the numerical solution of 2D and 3D models that incorporate the morphological and interfacial membrane characteristics in the heat and mass transfer of the MD process using a multi-region approach with OpenFOAM. The predicted values were validated by comparison with experimental data from the literature for the DCMD configuration, PVDF membrane with different morphological characteristics, and flat and hollow fiber geometries. The results suggested that the morphology of the membranes influences the selection of the models for membrane effective thermal conductivity and tortuosity. For the membrane with sponge-like morphology, the combination of the parallel-resistance model for the effective thermal conductivity and the fractal tortuosity model based on the random distribution of spheres provided an RMSE (root mean square error) concerning the experimental data of 0.7 kg/(m^2.h). On the other hand, for the membrane with an asymmetric pore distribution and macro voids in its the cross-section (finger-like channels), it was found that the combination of the parallel-resistance model for effective thermal conductivity and the Euclidian tortuosity model for the random arrangement of highly interconnected pores provided the highest agreement between experimental and theoretical data, presenting RMSE of 1.4 kg/(m^2.h) regarding the experimental data.*
Keywords: *Direct contact membrane distillation; membrane effective thermal conductivity; membrane tortuosity; computational simulation*

1. INTRODUCTION

Direct Contact Membrane Distillation (DCMD) is a thermal separation process with the vapor pressure gradient acting as the driving force resulting from the temperature difference between the feed stream (hot stream) and the permeate (cold stream). These two liquid streams are intermediated by a microporous and hydrophobic membrane that allows only volatile components through the membrane pores, ensuring the separation of the volatile components from the non-volatile ones present in the feed stream (Mulder, 1996).

In the DCMD process, heat and mass transfers take place simultaneously. Heat is transferred both by conduction and vapor carried in the membrane pores because of the temperature difference at the membrane surfaces (Khayet, 2011). Modeling and simulation of the transport phenomena that occur in the membrane distillation process are required for the theoretical evaluation of transport mechanisms, parameters analysis, and the influence of their interactions on process efficiency.

As pointed out by Manawi *et al.* (2014) and Liu *et al.* (2019), studies related to the representation of membrane morphology (e.g., pore size distribution and membrane tortuosity), membrane hydrophobicity, and associated transport parameters (e.g., membrane effective thermal conductivity) are scarce in the literature. These studies are mandatory for increasing the representativeness of membrane morphological and interfacial characteristics in the modeling and simulation of the MD process.

In porous media, tortuosity is defined as the ratio between the true length of the diffusion path, resulting from the spatial distribution of the solid particles and the fluid phase, and the thickness of the porous medium (Sahimi, 2011). In its turn, the effective thermal conductivity of a porous medium is a function of the porosity and thermal conductivity of the fluid and solid phases of the material. In the MD process, these properties have a direct impact on mass and heat transfer through the membrane. Tortuosity affects distilled water production negatively due to its impact on the diffusional path of volatile species through the membrane pores and the effective thermal conductivity is directly related to the heat losses by conduction through the membrane, affecting the thermal efficiency of the process (Smith *et al.*, 2013 and Deshmukh *et al.*, 2018).

The tortuosity and the effective thermal conductivity are characteristic parameters that can be determined experimentally (García-Payo and Izquierdo-Gil, 2004; Li *et al.*, 2014; Manickam *et al.*, 2014, and Huang and Reprogle, 2019). However, the thin thickness and compressibility of the porous matrix of the membrane structure are factors that can lead to experimental errors in the measurements of these parameters (Zhang *et al.*, 2012).

In the theoretical determination of the tortuosity, it has been usually assumed that this parameter depends on the pore geometry and the porosity of the medium. A diversity of mathematical models can be found in the literature for calculating tortuosity. These models can be inferred from the membrane pore geometry (Euclidean and fractal approaches) or deduced from analytical solutions of diffusional models (Boudreau, 1996; Iversen *et al.*, 1997; Shen and Chen, 2007; Ghanbarian *et al.*, 2013). Given the diversity of mathematical models for calculating the tortuosity of porous materials, Kim *et al.* (2021) evaluated 11 models, between Euclidean and fractal geometry approaches, which have been usually used in the literature for calculating the tortuosity of porous systems. Despite the number of models evaluated by Kim *et al.* (2021), some models often used in MD theoretical studies were not covered in that study, such as the model developed by Beeckman (1990) for modeling the tortuosity of pores highly interconnected in catalyst diffusion and used by Kim (2014); and the model derived from Bruggeman's correlation for randomly distributed spherical or cylindrical polymer structures, which was employed by Ismail *et al.* (2021). Therefore, the comparative analysis of the fitted models to the experimental data of the MD process is pertinent for greater study coverage.

Regarding the mathematical models for calculating membrane effective thermal conductivity, the parallel resistance model has been the most widely used in the literature for calculating the effective thermal conductivity of membranes used in desalination processes. This model represents an upper bound and assumes that the solid and fluid phases of the membrane domain are aligned parallel to the heat flux (Lawson and Lloyd, 1997; Khayet *et al.*, 2002; Hwang *et al.*, 2011; Andrjesdóttir *et al.*, 2013; Lisboa *et al.*, 2021). At the other extremity, representing a lower bound, the series resistance model has also been used to determine the effective thermal conductivity assuming that the fluid and solid phases are oriented perpendicular to the heat flow (Phattaranawik *et al.*, 2003; Chang *et al.*, 2015; Soukane *et al.*, 2017).

Bearing in mind that the parallel and series resistance models represent limiting cases for membrane geometric representation, García-Payo and Izquierdo-Gil (2004) and Hitsov *et al.* (2015) suggest the use of Maxwell's model (type I) for high porosity materials (>60%) because this model is not restricted to a limiting geometric case. In Maxwell's model (type I), it is assumed that the porous matrix can be represented by spherical inclusions of solid particles distributed in the fluid phase, under the assumption that the inclusions of the dispersed component are not in contact with the neighboring inclusions (Sundén, 2013). In theoretical studies of the desalination via membrane distillation process, the Maxwell (type I) model has already been used in the studies by Kim *et al.* (2014) and Lisboa *et al.* (2019).

The variety of models for estimating the effective thermal conductivity in porous media has motivated studies to evaluate the influence of selecting different models available in the literature, such as the studies by Phattaranawik *et al.* (2003), Huang e Reprogle (2019) and Ismail *et al.* (2021) that investigated the use of over one model option for calculating the membrane's effective thermal conductivity. The consideration of the dry air thermal conductivity for the fluid phase or the requirement of a previously known weighting factor for combining the models were factors that may have influenced their results.

In this context, the present study seeks to investigate the predictive ability of different models of effective thermal conductivity (parallel, series and Maxwell I) and tortuosity (Euclidean and fractal approach) commonly used in the literature to represent the effective and morphological characteristics of the membrane used in a DCMD desalination process. It thus aims to clarify the relationships between these models and the structure and morphology of these membranes. The different models of effective thermal conductivity and membrane tortuosity were evaluated using 2D (flat membrane) and 3D (hollow fiber membrane) models that incorporate the membrane morphological and interfacial properties in the heat and mass transfer analysis of the membrane distillation process. The numerical solution of the mathematical models was achieved with the finite volume method using OpenFOAM® (Jasak, 1996, 2009, Greenshields, 2011). The values derived from the simulations have been validated by comparison with experimental data from the literature for the DCMD configuration, PVDF membrane, with different morphological and structural characteristics, and flat (Yang *et al.*, 2014) and hollow fiber (Wang *et al.*, 2008) geometries.

2. MATHEMATICAL MODELLING

2.1. Fluid domain

The mass, momentum, and energy equations were solved for the feed and permeate fluid regions assuming the following simplifying hypotheses: Newtonian and thermal conductor Fourier fluid, with volumetric forces and viscous dissipation neglected. Moreover, incompressible laminar flow and steady-state regime were adopted. Regarding transport and thermophysical properties, all of them are considered temperature-dependent variables for a given NaCl input concentration.

2.2. Membrane domain

The Dusty-Gas model (Lawson e Lloyd, 1997) was adopted to model the mass transfer through the membrane domain, despite its known restriction for isothermal transport. Therefore, no species conservation equations were solved for this region, which is assumed as a solid region in which only thermal conduction, in steady-state regime, is the relevant transport mechanism. Nonetheless, the vaporization and condensation phenomena, in the feed and permeate stream, respectively, are accounted for in the interface membrane-side regions as source terms.

Therefore, the energy conservation equation for the membrane domain takes the form:

$$\nabla \cdot \left(k_{eff} \nabla T_m \right) = \begin{cases} \pm \dfrac{j_w h_{vap}(T_m)}{\delta_{\text{interface}}}, & \text{membrane interfaces} \\ 0, & \text{membrane bulk} \end{cases} \tag{1}$$

where: k_{eff} is the effective thermal conductivity, T_m is the membrane temperature field, j_w is the local distillate mass flux through the membrane region, h_{vap} is the latent heat. $\delta_{interface}$ is the membrane interface thickness, which is evaluated as an equivalent height of the portion of the pore volume that would be occupied by the liquid at the pore channel entrance, being approximated as the volume of a spherical cap (Liu *et al.*, 2019). According to this approach, for the flat and hollow-fiber PVDF membranes studied, the values 0,040 μm and 0,015 μm were obtained, respectively. It is worth mentioning that for these interface regions, the thermal conductivity of liquid water is used in the effective conductivity model instead of the vapor one.

By adopting the Dusty-Gas model, Dalton's law, neglecting air mass flux inside the pores, and considering the increase in the interface surface area due to the membrane hydrophobicity associated with the capillary depression, the local distillate mass flux is evaluated as:

$$j_w = C_{hidrophob} \frac{M_w D_{wa}}{R T_m \delta_{appa}} \ln\left(\frac{D_{wa} - D_{eff}\, p^v_{fd}}{D_{wa} - D_{eff}\, p^v_{pm}} \right) \tag{2}$$

$$C_{hidrophob} = \frac{2}{1 + \sin(\theta)} \tag{3}$$

$$\delta_{appa} = \begin{cases} \delta - \left(\delta_{\text{interf\_f}} + \delta_{\text{interf\_p}} \right), & \text{for the flat membrane} \\ \left(r_l + \delta_{\text{interf\_p}} \right) \ln\left(\dfrac{r_s - \delta_{\text{interf\_f}}}{r_l + \delta_{\text{interf\_p}}} \right), & \text{for the hollow-fiber membrane} \end{cases} \tag{4}$$

where $C_{hidrophob}$ is a surface correction factor for the permeate mass flux that accounts for the hydrophobicity degree, which is related to the water contact angle, θ, according to (Liu et al., 2019), which assumes the Wenzel's wetting state. Additionally, due to this increase on the interfacial surface, the distance between the two liquid/vapor interfaces is reduced, so the apparent membrane thickness (δ_{appa}) was also introduced in the mass flux equation. δ_{interf_f} is the feed-side interface thickness, δ_{interf_p} is the permeate-side interface thickness, and r_s and r_l are the external and internal radius of the hollow-fiber membrane, respectively.

M_w is water molecular weight, T_m is the mean absolute temperature inside the pores, R is the universal gas constant, δ_{appa} is the apparent membrane thickness and δ is the real membrane thickness, and $p_{fd}{}^v$ and $p_{pm}{}^v$ are the vapor pressures at the interface of the feed- and permeate-side with the membrane. D_{wa} is the molecular diffusion coefficient of water in the air inside the pores, D_{eff} is the effective diffusion coefficient, related to the Knudsen diffusivity, $D^k{}_w$, as:

$$D_{wa} = \frac{\varepsilon}{\tau} P D_m(T) \tag{5}$$

$$D_{eff} = \frac{D_w^k D_{wa}}{D_{wa} + P D_w^k} \tag{6}$$

$$D_w^k = \frac{\varepsilon d_p}{3\tau}\sqrt{\frac{8RT}{\pi M_w}} \tag{7}$$

where D_m is the molecular diffusion coefficient, P is the absolute pressure inside the pores, ε is the membrane porosity, τ is the membrane tortuosity and d_p is the membrane pore diameter.

2.3. Effective thermal conductivity and tortuosity models

Table 1 shows the effective thermal conductivity and tortuosity models usually cited in the literature (Andrjesdóttir et al., 2013; Kim, 2014; Eykens et al., 2016; Lisboa et al., 2019; Ismail et al., 2021) and evaluated in the present work.

Table 1. **Membrane's effective thermal conductivity, k_{eff}, and tortuosity, τ, models analyzed.**

Effective thermal conductivity "k_{eff}"		**Tortuosity "τ"**	
$k_{eff} = (1-\varepsilon)k_s + \varepsilon k_f$	(8)	$\tau = \dfrac{\varepsilon}{\left[1-(1-\varepsilon)^{1/3}\right]}$	(11)
$k_{eff} = \left[\dfrac{\varepsilon}{k_f} + \dfrac{(1-\varepsilon)}{k_s}\right]^{-1}$	(9)	$\tau = \dfrac{(2-\varepsilon)^2}{\varepsilon}$	(12)
$k_{eff} = k_f\left[\dfrac{1+(1-\varepsilon)2\beta_{s-f}}{1-(1-\varepsilon)2\beta_{s-f}}\right]$	(10)	$\tau = \dfrac{1}{\sqrt{\varepsilon}}$	(13)
$\beta_{s-f} = \left(\dfrac{k_s}{k_f}-1\right)\Big/\left(\dfrac{k_s}{k_f}+2\right)$		$\tau = \dfrac{1}{\varepsilon}$	(14)
		$\tau = \varepsilon^{1-D_T/(2-D_T)}$	(15)

k_f is the fluid phase thermal conductivity
k_s is the solid phase thermal conductivity
ε is the membrane porosity
D_T is the fractal dimension
d_f is the micropore fractal surface dimension

The parallel-resistance model (thermal conductivity in series, Eq. 8) is the most used effective thermal conductivity model, followed by series-resistance (thermal conductivity in parallel, Eq. 9) and the Maxwell I model, Eq. 10, (Phattaranawik et al., 2003; García-Payo e Izquierdo-Gil, 2004; Hitsov et al., 2015; Huang e Reprogle, 2019). In all these models, the fluid thermal conductivity in the bulk membrane, k_f, is made equal to the water vapor thermal conductivity, which is considered a temperature-dependent property. As previously mentioned, for the interface regions, however, the liquid water thermal conductivity is used.

For the tortuosity property, the first model described in Table 1 (Eq. 11) was developed by (Beeckman, 1990; Kim, 2014) from analytical solutions to the diffusion problem in heterogeneous catalysts, considering it a porous media with randomly interconnected pores. The second model (Eq. 12) is based on a Euclidian approach for a porous system represented by an ordered cubic lattice (Mackie e Meares, 1955). The last three models (Eqs. 13-15) are based on fractal theory. Tortuosity models described by Eqs. (13) e (14) are related to the Brugemman's correlation for porous media with pores randomly distributed within a solid matrix characterized by obstructions in the spherical or cylindrical format (Elias-Kohav, *et al.*, 1991; Iversen *et al.*, 1997; Tjaden *et al.*, 2016; Kim *et al.*, 2021). The model described by Eq. (15) was developed by Liu e Nie (2001), where the fractal dimension, D_T, and the micropore fractal surface dimension, d_f, can be found in the work of Xiao *et al.* (2019).

3. SOLUTION METHODOLOGY

The governing conservation equations were discretized and solved by the finite volume method with the OpenFOAM® open-source code. Hexaedrical meshes with 105.000 elements, for the flat membrane module, and with 474.000 elements, for the hollow-fiber membrane module were used to show the numerical results. A thorough convergence studies were performed to guarantee the accuracy of the results, and that the meshes in the interface regions were refined to a degree such that their elements had a thickness of approximately 1% of the membrane thickness. The simulations were carried out considering steady-state regime with relative error criteria of 10^{-6} for the residual of all the governing equations.

3.1. Geometries and boundary conditions

For both geometries analyzed, the flat membrane module (Figure 1) and the hollow-fiber membrane module (Figure 2), prescribed inlet velocity and temperature were set for the fluid domains, with the outlet pressure equal to the atmospheric pressure. Impermeability and non-slip boundary conditions are applied to the fluid streams at the membrane interfaces. On the other hand, since the hollow-fiber module is assumed as a semi-infinite domain, an external pseudo-wall is adopted where a slip boundary condition is employed for the velocity field and a null flux boundary condition is used for the temperature. Adiabatic conditions are applied to all other walls. Specifically, for the energy equation, a mapped condition was used for liquid/membrane interfaces. This guarantees that temperature and heat flux are the same on both sides of the membrane interface (stream-membrane).

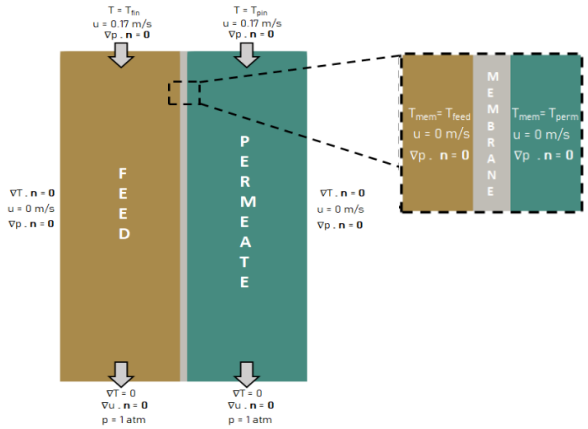

Figure 1 – **Flat plane membrane module and its boundary conditions.**

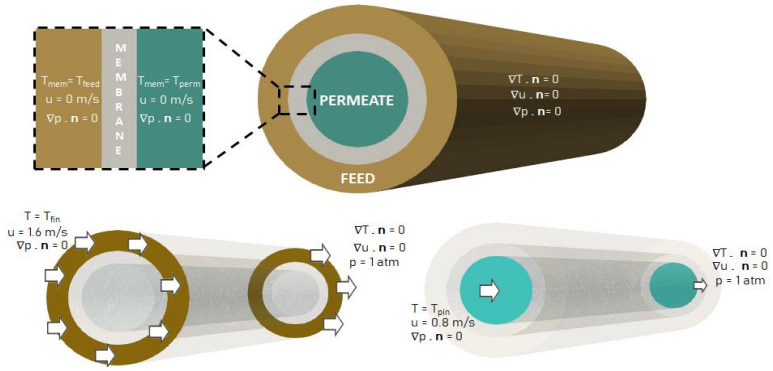

Figure 2 – **Hollow fiber membrane module and its boundary conditions.**

4. RESULTS AND DISCUSSION

The parametric analysis and validation of the proposed model were performed by comparison with the experimental distilled water flux data reported in the studies of Wang *et al.* (2008) and Yang *et al.* (2014) for hydrophobic PVDF (polyvinylidene fluoride) membranes of hollow and flat fiber geometries, respectively. The characteristics of the membranes and operating conditions used in this study are presented in Table 2.

Table 2. **Operational conditions and membranes characteristics of flat and hollow-fibers DCMD modules.**

Parameter	**DCMD Module**	
	Flat membrane Yang *et al.* (2014)	**Hollow-fiber membrane** Wang *et al.* (2008)
Mean pore diameter (d_p)	0.22 µm	0.16 µm
Membrane thickness (δ)	125 µm	110 µm
Membrane porosity (ε)	75%	73.8%
Water contact angle (θ)	130.2°	112°
Number of membranes/module (N_{fbr})	1	30 *
Effective membrane area	30 cm^2	150 cm^2
Feed inlet temperature	54 - 69°C	30 - 80°C
Feed inlet velocity	0.17 m/s	1.6 m/s
Permeate inlet temperature	21.1 °C	17.5 °C
Permeate inlet velocity	0.17 m/s	0.8 m/s
NaCl feed concentration (wt%)	4.0%	3.5%
Vessel radius (r_v)	---	4.7625 mm
Membrane length (L)	10 cm	20 cm

* Provided by Kim (2014).

The following figures illustrate the comparisons between the experimental data and the predicted values of water distillate flux for the two membrane geometries studied, taking into account different combinations of effective thermal conductivity and tortuosity models listed in Table 1.

Figures 3a-c illustrate some comparisons of the water distillate mass flux among simulated results and experimental data from Yang *et al.* (2014), for the flat membrane geometry. The theoretical results were achieved by considering all combinations of the five tortuosity models and the effective thermal conductivity models of resistance in series, Maxwell (type I), and resistance in parallel, respectively.

It can be noted that, for the flat membrane (with a sponge-like morphology), the tortuosity models based on fractal theory, Eqs. (13)-(15), provided better fits between simulated and experimental data, in particular, when combining these tortuosity models with the parallel resistance model, (Eq. 8), for the effective thermal conductivity (Elias-Kohav *et al.*, 1991; Iversen *et al.*, 1997; Tjaden *et al.*, 2016).

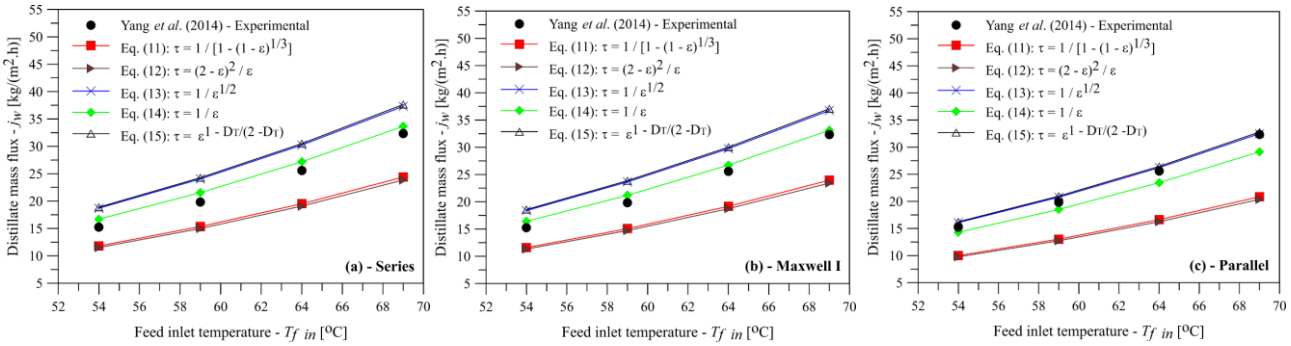

Figure 3. **Distillate mass flux for the flat membrane module, for different tortuosity models, and the following effective thermal conductivity models: (a) series - Eq.9, (b) Maxwell I - Eq.10 and (c) parallel - Eq.8.**

Based on the theoretical results obtained, it can be inferred that the combination of the parallel resistances model for the membrane effective thermal conductivity, Eq. (8), and the fractal tortuosity model that considers randomly distributed pores within a solid matrix characterized by obstructions with a spherical shape, Eq. (13), provided the best fitting of the simulated data to the experimental values, with a RMSE (root mean square error) value from the experimental data equal to 0,7 kg/(m^2.h) and an absolute pointwise relative deviation less than 5.5%, as presented in Table 3.

Table 3. **Relative deviation and RMSE of simulated distillate flux from experimental for the flat membrane module using different tortuosity and effective thermal conductivity models**

T_{fin} (°C)	Experimental Distillate flux Yang *et al.* (2014) (kg/m²h)	Relative deviation [%]				
		Tortuosity Model				
		Euclidian models		Fractal models		
		Eq. (11)	Eq. (12)	Eq. (13)	Eq. (14)	Eq. (15)
	θ=130.2°	Model of resistances in series – Eq. 9				
54	15.2	-22.6%	-24.4%	22.7%	9.6%	23.8%
59	19.8	-22.6%	-24.4%	21.3%	8.7%	22.4%
64	25.6	-23.7%	-25.4%	18.2%	6.3%	19.3%
69	32.3	-24.6%	-26.2%	15.4%	4.1%	16.4%
RMSE [kg/(m².h)]		5.7	6.1	4.4	1.5	4.6
	θ=130.2°	Maxwell I model – Eq. 10				
54	15.2	-24.0%	-25.8%	20.6%	7.7%	21.8%
59	19.8	-24.0%	-25.8%	19.3%	6.8%	20.4%
64	25.6	-25.0%	-26.7%	16.3%	4.5%	17.4%
69	32.3	-25.9%	-27.5%	13.7%	2.5%	14.6%
RMSE [kg/(m².h)]		6.1	6.5	3.9	1.1	4.2
	θ=130.2°	Model of resistances in parallel – Eq. 8				
54	15.2	-34.4%	-36.0%	5.5%	-6.2%	6.5%
59	19.8	-34.2%	-35.8%	4.7%	-6.6%	5.7%
64	25.6	-35.0%	-36.5%	2.5%	-8.3%	3.4%
69	32.3	-35.5%	-37.0%	0.5%	-9.8%	1.4%
RMSE [kg/(m².h)]		8.4	8.8	0.7	2.1	0.9

Furthermore, according to those results in Table 3, it seems that the effective thermal conductivity model does not show a dominant role in the distillate mass flux for this kind of membrane morphology (to which the fractal tortuosity models are the most suitable), as any of the effective thermal conductivity models studied could be, at first, employed. This behavior highlights the needing for heat transfer parameter analysis (such as heat flux and thermal efficiency) for a proper choicer of a membrane effective thermal conductivity model.

Figures 4a-c compare the water distillate mass flux simulated values for the hollow fiber membrane geometry with the experimental data from Wang *et al.* (2008). For this analysis, the 5 tortuosity models were analyzed, considering the effective thermal conductivity models of resistances in series, Maxwell (type I), and resistances in parallel, respectively, as previously performed for the flat geometry membrane.

Differently from the flat membrane, the cross-section of the hollow fiber membrane presents a morphology where asymmetric pore distribution with internal macro-voids (finger-like channels) are characteristics. The results presented in Figures 4a-c and Table 4 show that Euclidian tortuosity models are satisfactory to represent this kind of membrane morphology. In particular, the model developed by Beeckman (1990), Eq. (11), for a random arrangement of highly interconnected pores is the most appropriate for the description of the distillate mass flux, specifically when associated with the model of resistances in parallel for the membrane effective thermal conductivity, Eq. (8). This combination provided the highest approximation between theoretical and experimental data, producing a RMSE value of the deviation from the experimental data equal to 1.4 1.4 kg/(m^2.h), despite an absolute pointwise relative deviation of around 25%, as presented in Table 4.

As observed for the flat membrane, the effective thermal conductivity model again does not show a dominant role in the distillate mass flux for this kind of membrane morphology, since any of the evaluated effective thermal conductivity models could, in principle, also be employed.

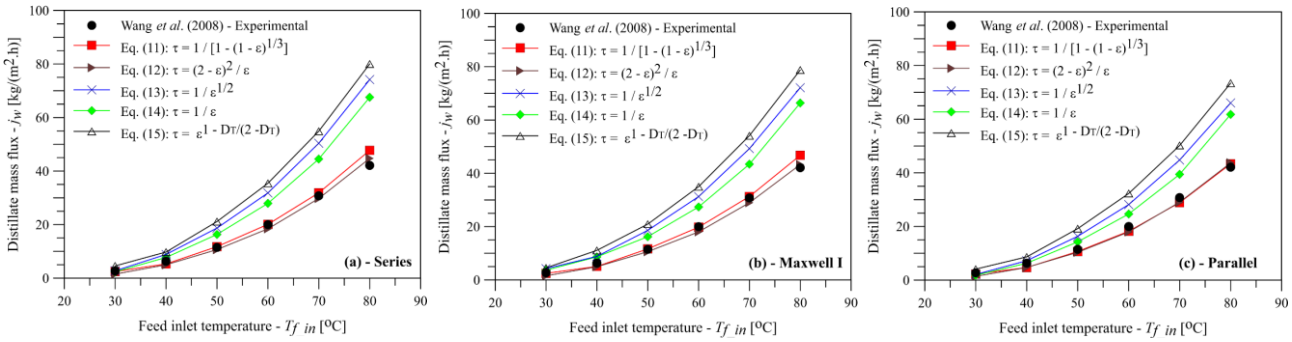

Figure 4. **Distillate mass flux for the hollow-fiber membrane module, for different tortuosity models, and the following effective thermal conductivity models: (a) series - Eq.9, (b) Maxwell I - Eq.10 and (c) parallel - Eq.8.**

As previously mentioned, the differences between the results obtained with different combinations of the effective thermal conductivity and membrane tortuosity models are certainly associated to the structural and morphological differences of each of the membranes employed.

Therefore, for the PVDF membrane of flat geometry with sponge-like characteristics (scanning electron microscopy images, SEM, Figure S1A and S1B in Appendix A of Yang *et al.* (2014)), the morphological and structural characteristics associated with pore size and pore distribution are best represented by the fractal random distribution tortuosity model with the spherical shaped diffusion obstructions (Eq. 13) combined with the parallel thermal resistances effective thermal conductivity model (Eq. 8).

On the other hand, for the PVDF hollow fiber membrane, which has macro-voids (finger-like channels) in its internal part and asymmetric pores on the inner and outer surfaces (scanning electron microscopy image, SEM, Figure 2 of Wang *et al.* (2008)), the results show that the tortuosity model developed by Beeckman (1990) (Eq. 11) describes well the distillate mass flux, especially when associated with the parallel resistance model for the effective thermal conductivity (Eq. 8).

In summary, the results presented in this study have shown that for adequate modeling of the phenomenon of desalination by direct contact membrane distillation (DCMD), the choice of the effective thermal conductivity model and, especially, the tortuosity model should always be associated with the morphology and structure of the membrane used, since different morphologies and internal structures of these membranes lead to distinct diffusion and conduction paths through them, so that a tortuosity model may represent well these phenomena for a type of membrane, but poorly for another membrane with different morphological characteristics. Even though the results indicated that the combination of the respective tortuosity models and the parallel resistances model for membrane effective thermal conductivity provided the best fit to the experimental data, the analysis of the heat transfer parameters might be mandatory for a proper selection for the membrane effective thermal conductivity model.

Table 4. **Relative deviation and RMSE of simulated distillate flux from experimental for the hollow-fiber membrane module using different tortuosity and effective thermal conductivity models**

T_{fin} (°C)	Experimental Distillate flux Wang *et al.* (2008) (kg/m²h)	Relative deviation [%]				
		Tortuosity Model				
		Euclidian models		Fractal models		
		Eq. (11)	Eq. (12)	Eq. (13)	Eq. (14)	Eq. (15)
	θ=112°	Model of resistances in series – Eq. 9				
30	2.7	-8,0%	-44.0%	1.5%	-12.2%	69.2%
40	6.3	-15,6%	-20.5%	41.0%	22.8%	55.2%
50	11.5	2,3%	-7.2%	62.4%	42.0%	83.6%
60	20.0	0,8%	-7.7%	59.5%	40.0%	77.5%
70	30.8	3,6%	-3.2%	63.9%	44.7%	78.5%
80	42.1	13,4%	6.3%	76.2%	60.5%	90.2%
RMSE [kg/(m².h)]		2.4	1.5	16.4	12.4	19.9
	θ=112°	Maxwell I model – Eq. 10				
30	2.7	-8,7%	-42.7%	56.7%	36.1%	68.2%
40	6.3	-19,7%	-21.0%	40.6%	37.7%	76.1%
50	11.5	1,1%	-8.0%	61.5%	41.0%	81.7%
60	20.0	-0,8%	-9.7%	56.6%	37.3%	75.3%
70	30.8	1,8%	-5.8%	60.2%	41.2%	76.0%
80	42.1	11,1%	2.9%	71.4%	57.8%	87.2%
RMSE [kg/(m².h)]		2.0	1.4	15.5	11.8	19.3
	θ=112°	Model of resistances in parallel – Eq. 8				
30	2.7	-17.6%	-48.0%	-22.7%	-33.3%	52.0%
40	6.3	-25.5%	-24.7%	14.9%	-0.1%	37.6%
50	11.5	-7.5%	-9.8%	42.0%	24.0%	66.8%
60	20.0	-8.7%	-10.0%	41.0%	23.5%	61.8%
70	30.8	-6.0%	-5.5%	45.7%	28.3%	63.2%
80	42.1	3.0%	3.9%	57.0%	46.8%	74.5%
RMSE [kg/(m².h)]		1.4	1.6	12.0	9.1	16.2

5. CONCLUSIONS

The results reported in this study show that membrane cross-section morphology and pore size and distribution are factors that should be considered during the selection of the membrane effective thermal conductivity and tortuosity models. For the membrane with sponge-like morphology along the transverse direction of the flat membrane, there was a better fit of the theoretical distillate flux data to the experimental data from the literature by combining the resistances in parallel effective thermal conductivity model and the tortuosity model that assumes a random distribution of spherically shaped solid material, providing resistance to diffusive transport. This model combination provided a RMSE around 0.7 kg/(m^2.h).

Regarding the membrane that had macro-voids in the cross-section (hollow fiber membrane) and asymmetric pore size and distribution, it was found that the combination of the resistance in parallel model for effective thermal conductivity and Beeckman's (1990) tortuosity model for a random arrangement of highly interconnected pores provided the highest agreements between experimental and theoretical data, yielding a RMSE equal to 1.4 kg/(m^2.h).

Therefore, these results suggested that the morphological anisotropy of the porous membrane affected the model selection. The results reported show that membrane cross-section morphology and pore size and pore distribution are factors that should be considered during the selection of a membrane effective thermal conductivity and of a tortuosity models. In general, at least for the distillate mass flux, it seems that fractal-based tortuosity models represent well membranes with sponge-like morphology along all their cross-section (as the flat membrane analyzed), whereas Euclidian tortuosity models are the best choice for membranes membrane that present macro-voids in the cross-section and asymmetric pore size and distribution (as the hollow fiber membrane studied).

Finally, the results presented also suggest that a proper choice of effective thermal conductivity and tortuosity models should be based on both results of thermal variables (like the heat transported by conduction, and the thermal efficiency) and mass transfer parameters (like distillate mass flux), since, at a first glance, a crossing effect between the selected models may be present. In other words, an effective thermal conductivity model may not be adequate for predicting the thermal parameters, however, its effect on mass flux parameters can be minimized by a representative tortuosity model.

6. ACKNOWLEDGMENTS

Partial funding by Petrogal Brasil Project Nos. GALP 38, and the sponsoring agencies CNPq, FAPERJ, and CAPES/PROCAD Defesa, are gratefully acknowledged. P.R. Júnior acknowledges the engineers Natalia Correia de Sá, Eduardo Paiva dos Santos and Filipe Eduardo Cunha de Souza for their help in the execution of the computational code developed.

7. REFERENCES

ANDRJESDÓTTIR, Ó., ONG, C. L., NABAVI, M., PAREDES, S., KHALIL, A., MICHEL, B., POULIKAKOS, D., 2013. "An experimentally optimized model for heat and mass transfer in direct contact membrane distillation", *International Journal of Heat and Mass Transfer*, Vol. 66, pp. 855–867. DOI: 10.1016/j.ijheatmasstransfer.2013.07.051.

BEECKMAN, J. W., 1990. "Mathematical Description of the heterogeneous materials", *Chemical Engineering Sciences*, Vol. 45, No. 8, pp. 2603–2610.

BOUDREAU, B. P., 1996. "The diffusive tortuosity of fine-grained unlithified sediments", **G***eochimica et Cosmochimica Acta*, Vol. 60, No. 16, pp. 3139–3142. DOI: 10.1016/0016-7037(96)00158-5.

CHANG, H., HSU, J., CHANG, C., HO, C., CHENG, T., 2015. "Simulation study of transfer characteristics for spacer-filled membrane distillation desalination modules ", *Applied Energy*, p. 1–13. DOI: 10.1016/j.apenergy.2015.12.030.

DESHMUKH, A., BOO, C., KARANIKOLA, V., LIN, S., STRAUB, A. P., TONG, T., WARSINGER, D. M., ELIMELECH, M., 2018. "Membrane distillation at the water-energy nexus: limits, opportunities, and challenges", *Energy & Environmental Science*, Vol. 11, No. 5, pp. 1177–1196. DOI: 10.1039/C8EE00291F.

ELIAS-KOHAV, T., MOSHE, S., AVNIR, D., 1991. "Steady-state diffusion and reactions in catalytic fractal porous media", *Chemical Engineering Science*, Vol. 46, No. 11, pp. 2787–2798. DOI: 10.1016/0009-2509(91)85148-Q.

EYKENS, L., De SITTER, K., DOTREMONT, C., PINOY, L., Van der BRUGGEN, B., 2016. "Characterization and performance evaluation of commercially available hydrophobic membranes for direct contact membrane distillation", *Desalination*, Vol. 392, pp. 63-73. DOI: 10.1016/j.desal.2016.04.006.

GARCÍA-PAYO, M. C., IZQUIERDO-GIL, M. A., 2004. "Thermal resistance technique for measuring the thermal conductivity of thin microporous membranes", *Journal of Physics D: Applied Physics*, Vol. 37, No. 21, pp. 3008–3016. DOI: 10.1088/0022-3727/37/21/011.

GHANBARIAN, B., HUNT, A. G., SAHIMI, M., 2013. "Percolation Theory Generates a Physically Based Description of Tortuosity in Saturated and Unsaturated Porous Media", *Soil Science Society of America Journal*, Vol. 77, No. 6, pp. 1920–1929. DOI: 10.2136/sssaj2013.01.0089.

GREENSHIELDS, C., 2011 "OpenFOAM The OpenFOAM Foundation User Guide".

HITSOV, I., MAERE, T., DE SITTER, K., DOTREMONT, C., NOPENS, I., 2015. "Modelling approaches in membrane distillation: A critical review", *Separation and Purification Technology*, Vol. 142, pp. 48–64. DOI: 10.1016/j.seppur.2014.12.026.

HUANG, F. Y. C., REPROGLE, R., 2019. "Thermal Conductivity of Polyvinylidene Fluoride Membranes for Direct Contact Membrane Distillation", *Environmental Engineering Science*, Vol. 00, No. 00, pp. 1–11. DOI: 10.1089/EES.2018.0349.

HWANG, H. J., HE, K., GRAY, S., ZHANG, J., MOON, I. S., 2011. "Direct contact membrane distillation (DCMD): Experimental study on the commercial PTFE membrane and modeling", *Journal of Membrane Science*, Vol. 371, No. 1–2, pp. 90–98. DOI: 10.1016/j.memsci.2011.01.020.

ISMAIL, M. S., MOHAMED, A. M., POGGIO, D., POURKASHANIAN, M., 2021. "Direct contact membrane distillation: A sensitivity analysis and an outlook on membrane effective thermal conductivity", *Journal of Membrane Science*, v. 624, n. January, p. 119035. DOI: 10.1016/j.memsci.2020.119035.

IVERSEN, S. B., BHATIA, V. K., DAM-JOHANSEN, K., JONSSON, G., 1997. "Characterization of microporous membranes for use in membrane contactors", *Journal of Membrane Science*, Vol. 130, No. 1–2, pp. 205–217. DOI: 10.1016/S0376-7388(97)00026-4.

JASAK, H. "Error Analysis and Estimation for the Finite Volume Method with Applications to Fluid Flows". Ph.D. Thesis. Department of Mechanical Engg. University of London, 1996.

JASAK, H., 2009. "OpenFOAM: Open source CFD in research and industry", *International Journal of Naval Architecture and Ocean Engineering*, Vol. 1, No. 2, pp. 89–94. DOI: 10.3744/JNAOE.2009.1.2.089.

KHAYET, M., GODINO, M. P., MENGUAL, J. I., 2002. "Thermal boundary layers in sweeping gas membrane distillation processes", *AIChE Journal*, Vol. 48, No. 7, pp. 1488–1497. DOI: 10.1002/aic.690480713.

KHAYET, M., 2011 "Membranes and theoretical modeling of membrane distillation: A review", *Advances in Colloid and Interface Science*, Vol. 164, No. 1–2, pp. 56–88. DOI: 10.1016/j.cis.2010.09.005.

KIM, A. S., 2014. "Cylindrical cell model for direct contact membrane distillation (DCMD) of densely packed hollow fibers", *Journal of Membrane Science*, Vol. 455, pp. 168–186. DOI: 10.1016/j.memsci.2013.12.067.

KIM, W. J., CAMPANELLA, O., HELDMAN, D. R., 2021. "Predicting the performance of direct contact membrane distillation (DCMD): Mathematical determination of appropriate tortuosity based on porosity", *Journal of Food Engineering*, Vol. 294, pp. 110400. DOI: 10.1016/j.jfoodeng.2020.110400.

LAWSON, K. W., LLOYD, D. R., 1997. "Membrane distillation". *Journal of Membrane Science*. Vol. 124, pp. 1-25.

LI, Z., PENG, Y., DONG, Y., FAN, H., CHEN, P., QIU, L., JIANG, Q., 2014. "Effects of thermal efficiency in DCMD and the preparation of membranes with low thermal conductivity", *Applied Surface Science*, Vol. 317, pp. 338–349. DOI: 10.1016/j.apsusc.2014.07.080.

LISBOA, K. M., BUSSON, D. M., NAVEIRA-COTTA, C. P., COTTA, R. M., 2021. "Analysis of the membrane effects on the energy efficiency of water desalination in a direct contact membrane distillation (DCMD) system with heat recovery", *Applied Thermal Engineering*, Vol. 182, pp. 116063. DOI: 10.1016/j.applthermaleng.2020.116063.

LISBOA, K. M., DE SOUZA, J. R. B., NAVEIRA-COTTA, C. P., COTTA, R. M., 2019. "Heat and mass transfer in hollow-fiber modules for direct contact membrane distillation: Integral transforms solution and parametric analysis", *International Communications in Heat and Mass Transfer*, Vol. 109, pp. 104373, 2019. DOI: 10.1016/j.icheatmasstransfer.2019.104373.

LIU, J.G., NIE, Y.F., 2001, "Fractal scaling of effective diffusion coefficient of solute in porous media," *Journal of Environmental Sciences*, vol. 13, No. 2, pp. 170-172.

LIU, J., WANG, Q., SHAN, H., GUO, H., LI, B., 2019. "Surface hydrophobicity based heat and mass transfer mechanism in membrane distillation", *Journal of Membrane Science*, Vol. 580, pp. 275–288. DOI: 10.1016/j.memsci.2019.01.057.

MACKIE, J. S., MEARES, P., 1955. "The diffusion of electrolytes in a cation-exchange resin membrane: I. Theoretical", In P*roceedings Royal Society London Math Phys Sci*, Vol. 232, No. 81191, pp. 498–509, 1955. DOI: 10.1246/nikkashi1921.58.819.

MANAWI, Y. M., KHRAISHEH, M., FARD, A. K., BENYAHIA, F., ADHAM, S., 2014. "Effect of operational parameters on distillate flux in direct contact membrane distillation (DCMD): Comparison between experimental and model predicted performance", *Desalination*, Vol. 336, No. 1, pp. 110–120. DOI: 10.1016/j.desal.2014.01.003.

MANICKAM, S. S., GELB, J., MCCUTCHEON, J. R., 2014. "Pore structure characterization of asymmetric membranes: Non-destructive characterization of porosity and tortuosity", *Journal of Membrane Science*, Vol. 454, pp. 549–554. DOI: 10.1016/J.MEMSCI.2013.11.044.

MULDER, M., 1996. *Basic Principles of Membrane Technology*. Kluwer Academic Publishers, Dordrecht, The Netherlands.

PHATTARANAWIK, J., JIRARATANANON, R., FANE, A. G., 2003. "Heat transport and membrane distillation coefficients in direct contact membrane distillation", *Journal of Membrane Science*, Vol. 212, No. 1–2, pp. 177–193. DOI: 10.1016/S0376-7388(02)00498-2.

SAHIMI, M., 2011. *Transport Modeling for Environmental Engineers and Scientists Nonlinear Mesoscopic Elasticity Essentials of Multiphase Flow in Porous Media*. 2nd Ed. Ed. WILEY-VCH, Weinheim, Germany.

SHEN, L., CHEN, Z., 2007. "Critical review of the impact of tortuosity on diffusion", *Chemical Engineering Science*, Vol. 62, No. 14, pp. 3748–3755. DOI: 10.1016/j.ces.2007.03.041.

SMITH, D. S., ALZINA, A., BOURRET, J., NAIT-ALI, B., PENNEC, F., TESSIER-DOYEN, N., 2013. "Thermal conductivity of porous materials", *Journal of Materials Research*, Vol. 28, No. 17, pp. 2260–2272. DOI: 10.1557/jmr.2013.179.

SOUKANE, S., NACEUR, M. W., FRANCIS, L., ALSAADI, A., GHAFFOUR, N., 2017. "Effect of feed flow pattern on the distribution of permeate fluxes in desalination by direct contact membrane distillation", *Desalination*, v. 418, pp. 43–59, 2017. DOI: 10.1016/j.desal.2017.05.028.

SUNDÉN, B., YUAN, J., 2013 "Evaluation of models of the effective thermal conductivity of porous materials relevant to fuel cell electrodes", *International Journal of Computational Methods and Experimental Measurements*, Vol. 1, No. 4, pp. 440–455. DOI: 10.2495/CMEM-V1-N4-440-455.

TJADEN, B., COOPER, S. J., BRETT, D. J., BRETT, D. J., KRAMER, D., SHEARING, P. R., 2016. "On the origin and application of the Bruggeman correlation for analysing transport phenomena in electrochemical systems", *Current Opinion in Chemical Engineering*, Vol. 12, pp. 44–51. DOI: 10.1016/j.coche.2016.02.006.

WANG, K. Y., CHUNG, T. S., GRYTA, M., 2008. "Hydrophobic PVDF hollow fiber membranes with narrow pore size distribution and ultra-thin skin for the fresh water production through membrane distillation", *Chemical Engineering Science*, Vol. 63, No. 9, pp. 2587–2594. DOI: 10.1016/j.ces.2008.02.020.

XIAO, B., WANG, W., ZHANG, X., LONG, G., FAN, J., CHEN, H., DENG, L., 2019. "A novel fractal solution for permeability and Kozeny-Carman constant of fibrous porous media made up of solid particles and porous fibers", *Powder Technology*, Vol. 349, pp. 92-98, DOI: 10.1016/J.POWTEC.2019.03.028.

YANG, C., LI, X. M., GILRON, J., KONG, D., YIN, Y., OREN, Y., LINDER, C., HE, T., 2014 "CF4 plasma-modified superhydrophobic PVDF membranes for direct contact membrane distillation", *Journal of Membrane Science*, Vol. 456, pp. 155–161, 2014. DOI: 10.1016/j.memsci.2014.01.013.

ZHANG, J., GRAY, S., LI, Jun-De., 2012. "Modelling heat and mass transfers in DCMD using compressible membranes", *Journal of Membrane Science*, Vol. 387–388, No. 1, pp. 7–16. DOI: 10.1016/j.memsci.2011.08.034.

8. AUTHORSHIP RESPONSIBILITY

The authors are solely responsible for the content of this work.